Electronic Supplementary Material (ESI) for Chemical Communications.
This journal is © The Royal Society of Chemistry 2017

**ELECTRONIC SUPPLEMENENTARY INFORMATION for**

# Synthesis and Structure of Synthetically Pure and Deuterated Amorphous (Basic) Calcium Carbonates

Hsiu-Wen Wang,[a]* Luke L. Daemen,[b] Joe Roback,[c] Michael C. Cheshire,[d] Michelle K. Kidder,[d] Andrew G. Stack,[d] Lawrence F. Allard,[e] Jörg Neuefeind,[b] Daniel Olds,[b] Jue Liu,[b] and Katharine Page[b]*

[a] Joint Institute for Neutron Sciences, the University of Tennessee/Oak Ridge National Laboratory, Oak Ridge, TN 37831; [b] Spallation Neutron Source, Oak Ridge National Laboratory, Oak Ridge, TN 37831; [c]Montana State University, Bozeman, MT 59715; [d] Chemical Sciences Division, Oak Ridge National Laboratory, Oak Ridge, TN 37831; [e] Materials Science and Technology Division, Oak Ridge National Laboratory, Oak Ridge, TN 37831.

## Supplementary Table:

**Table S1.** Summary of the spontaneous precipitation procedures published in the literature.

| no. | Prior reaction: concentration, pH*, and temperature | After mixing: $SI_c$ of the reacted solution at time zero‡, treatments following precipitation, and other comments | ref. |
|---|---|---|---|
| ***Rapid mixing (as soon as possible) method: spontaneous precipitation proceeds on a timescale of seconds*** | | | |
| *$CaCl_2$-$Na_2CO_3$-NaOH system: at all conditions pH is > 10 and $SI_c$ is estimated to be ≥ 2.5* | | | |
| *or, $CaCl_2$-$Na_2CO_3$ system: NaOH was omitted for a pH of 9.1-12; $SI_c$ is estimated to be > 2.6* | | | |
| [1] | Kojima et al. (1993): equivolume mixture of 0.1 M $CaCl_2$ and 0.1 M $Na_2CO_3$ + 0-3 M NaOH (pH 11-14) at 0 °C | $SI_c$ = 3.79-2.56 (for pH = 11-14) The solid was filtered and dried in a vacuum. ACC and ABCC phases were formed at pH 11.0-13.5 and 13.5-14.0, respectively. Effects of pH on temperature of crystallization were reported. | 1 |
| [2] | Koga et al. (1998): equivolume mixture of 0.1 M $CaCl_2$ and 0.1 M $Na_2CO_3$ + 0-2 M NaOH (pH 11.2-13.5) at 5 °C | $SI_c$ = 3.80-2.87 (for pH = 11.2-13.5) The precipitate was filtered, washed with acetone, and then dried in a vacuum for one day. ABCC is formed at pH > 13. At pH 11-13, there is a linear trend toward an increasingly exothermic crystallization reaction and temperature of crystallization with increasing pH. | 2 |
| [3] | equivolume mixture of 9 mM $CaCl_2$ and 9 mM $Na_2CO_3$ + 0.5 mM NaOH (pH 10.2) at 25 °C | $SI_c$ = 2.6 The precipitated colloidal phases were measured *in situ* with time-resolved small-angle X-ray scattering. Amorphous precipitates occur in well-defined spheres with a remarkable uniformity in size. | 3 |
| [4] | equivolume mixture of 0.02 M $CaCl_2$ and 0.02 M $Na_2CO_3$ + 0.2 M NaOH (pH* 13.14) at 25 °C | $SI_c$ = 2.79 The precipitate was vacuum filtered and rinsed with acetone to dry. This method is modified from Koga *et al.*[2] Structural modeling of ACC by Goodwin *et al.*[4] was completed on X-ray PDF data from this synthesis method. | 5 6 |
| [5] | equivolume mixture of 0.02 M $CaCl_2$ and 0.02 M $Na_2CO_3$ + 0.2 M NaOH (pH* 14.08-13.92) at ~0-4 °C | $SI_c$ = 2.50 (for pH* = 14.08 at 0 °C), 2.59 (for pH* = 13.92 at 4 °C) The precipitate was vacuum filtered, washed with acetone and vacuum dried overnight. Same method as described by Michel *et al.*[6] but reacted at lower temperatures (~0-4 °C). | 7 8 9 |
| [6] | equivolume mixture of 0.02 M $CaCl_2$ and 0.02 M $Na_2CO_3$ + 0.1 M NaOH (pH 12.8) at 25 °C | $SI_c$ = 2.90 The precipitate was vacuum filtered, rinsed with acetone, and dried further under soft vacuum in the presence of desiccant for 10-20 min. This method is adopted from Koga *et al.*[2] and Michel *et al.*[6]. | 10 |
| [7] | equivolume mixture of 0.013 M $CaCl_2$ and 0.013 M $Na_2CO_3$ + 0-0.16 M NaOH at 25 °C (pH = 11.2 for no | $SI_c$ = 2.81-2.54 (for pH = 11.2-13) The precipitate was vacuum-filtered (completed within 30 s of mixing), the solid was rinsed with isopropanol to remove remaining water and then quickly | 11 |

| | | | |
|---|---|---|---|
| | NaOH added; pH = 11.8, 12.5, 12.75, and 13 for 0.01, 0.04, 0.08, and 0.16 M NaOH added, respectively) | dried by blowing air over the solid. The corresponding X-ray PDFs indicate a subtle difference for amorphous samples obtain at different pH conditions. | |
| [8] | equivolume mixture of 0.02 M $CaCl_2$ and 0.02 M $Na_2CO_3$ (pH 9.8) at 25 °C | $SI_c$ = 2.75<br>The reported pH (9.8) for a 0.02 M $Na_2CO_3$ solution suggested that the solution was equilibrated with atmospheric $CO_2$. A fresh 0.02 M $Na_2CO_3$ solution should have pH of ~11. $SI_c$ thus calculated considers the equilibrium with atmosphere $CO_2$ and $O_2$. | 10 |
| [9] | equivolume mixture of 1 M $CaCl_2$ and 1 M $Na_2CO_3$ (pH* 12.02, 11.94, 11.62, 11.48) at 7.5, 10, 20, 25 °C, respectively | $SI_c$ = 4.97 (for pH* = 12.02 at 7.5 °C), 4.98 (for pH* = 11.94 at 10 °C), 4.94 (for pH* = 11.62 at 20 °C), 4.92 (for pH* = 11.48 at 25 °C)<br>pH of the carbonate solutions was varied via temperature. The reactions were followed *in situ* using time-resolved synchrotron-based energy dispersive-XRD and wide angle X-ray scattering. Ihli *et al.*[12] washed their precipitate with isopropanol, but also commented that synthetic ACC with long-term stability is only typically reported on precipitation from ethanol. | 12<br>13<br>14 |
| *$CaCl_2$-$(NH_4)_2CO_3$ system: pH of 9-11; $SI_c$ is estimated to be > 2.6* | | | |
| [10] | equivolume mixture of 0.01 M $CaCl_2$ and 0.01 M $Na_2CO_3$ (pH* 10.97) at 1 °C | $SI_c$ = 2.65<br>The precipitate was vacuum-filtered, washed with isopropanol, dried using flowing air, and stored in a sealed container. | 15 |
| [11] | equivolume mixture of 1 M $CaCl_2$ and 1 M $(NH_4)_2CO_3$ (pH 9.15) at 4 °C | $SI_c$ = 4.48<br>The precipitate was immediately filtered before washing with ethanol and drying over silica gel for 1h. ACC only shows extended stability when washed with ethanol, where the surface-bound $H_2O$ can be effectively displaced by ethanol. | 12<br>16 |
| *Hydrolysis of $(CH_3)_2CO_3$: Precipitation begins via adding base (NaOH) to the reaction solution, i.e., increase of pH* | | | |
| [12] | excess of $(CH_3)_2CO_3$ over $Ca^{2+}$:<br>0.8 vs. 0.2 volume ratio mixture of 0.0125 M $CaCl_2$ + 0.0625 M $(CH_3)_2CO_3$ (pH* 4.28) and 0.5 M NaOH at 25 °C | $SI_c$ = 1.71<br>The precipitate was recovered by centrifugation, then washed with acetone and dried under vacuum. ACCs occur as well-defined/narrow-size-distributed spheres. Xu *et al.*[17] washed their precipitates with acetone and ethanol. | 18<br>17<br>6<br>10 |
| [13] | equimolar ratio of $(CH_3)_2CO_3$ to $Ca^{2+}$:<br>0.02 M $CaCl_2$ + 0.02 M $(CH_3)_2CO_3$ (pH* 3.94, 3.92, 3.89) and 0.04 M NaOH at 15, 20, 30 °C, respectively | $SI_c$ = 2.80 (for pH* = 3.94 at 15 °C), 2.79 (for pH* = 3.92 at 20 °C), 2.78 (for pH* = 3.89 at 30 °C)<br>ACCs formed at high reaction temperatures systematically showed to be smaller in size. Note that precipitation under quiescent conditions can be achieved with the use of $(CH_3)_2CH_2(CO_3)$ as source of $CO_2$, because its hydrolysis is much slower. | 18 |
| ***Slow dosing (titration) method: spontaneous precipitation proceeds on a timescale of hours*** | | | |
| *$CaCl_2$-$Na_2CO_3$-$NaHCO_3$-NaOH system: pH of the carbonate solution is kept constant; $SI_c$ is estimated to be < 1.6* | | | |
| [14] | 10 mM $CaCl_2$ was added (10µL/min) to 10 mM $Na_2CO_3$-$NaHCO_3$ of pH 8.75-10. The pH is kept constant by titration with 10 mM NaOH. Reaction temperature is 24 °C. | $SI_c$ = ~1.37 (for pH = 8.75-9.25), ~1.51 (for pH 9.5), and ~1.55 (for pH 9.75 and 10.0)<br>Reaction is started via dosing calcium solution into the carbonate buffer ($Na_2CO_3$-$NaHCO_3$). pH and calcium potential are both monitored in order to calculate the amount of bound carbonate ions (as pre-nucleation clusters and post-nucleation precipitates) from constant-pH titration curves. In 2010, these authors reported a method to extract ACC from the reaction solutions, in which the solution was rapidly poured into an excess of ethanol, stirred for ~30 min, left standing for ~2 h, decanted and precipitate was centrifuged. The precipitate was washed with ethanol, isopropanol and acetone and eventually dried. The synthesis with pH 8.75 and 9.80 yielded pc-ACC and pv-ACC. | 19<br>20 |

* Carbonate solution with high pH value will quickly equilibrate with atmospheric $CO_2$, dropping the pH to ~9-10 if stored at ambient laboratory environments for several days. pH monitoring is thus critical when comparison is made for various synthetic A(B)CC materials reported in the literature. For pH values that are not specified in the publication (marked by pH*), the estimated value is calculated using

PHREEQC code[21] with llnl database. For the calculation, we assume fresh carbonate solutions without equilibrating with atmospheric $CO_2$ and $O_2$. Calculated pH error is about ± 0.3, depending on the chosen database.

‡ $SI_c$ = Saturation index with respect to calcite; this is a nominal value and is calculated using PHREEQC code[21] with llnl database.

**Table S2.** Stoichiometry composition of the samples

| samples* | wt. loss as % at 270 & 350°C | residual wt.% at 800°C† | calc. wt.% for composed species: $H_2O$ | $Ca(OH)_2$ | $CaCO_3$ | CaO† | stoichiometry, expressed as $Ca(OH)_{2x}(CO_3)_{1-x} \bullet nH_2O$* |
|---|---|---|---|---|---|---|---|
| p-A(B)CC (2h) | 11.33 & 1.25 | 50.86 | 11.33 | 5.14 | 83.53 | 50.69 | $Ca(OH)_{0.154}(CO_3)_{0.923} \bullet 0.696H_2O$ |
| p-A(B)CC (1h) | 15.47 & 1.19 | 49.02 | 15.47 | 4.89 | 79.64 | 48.32 | $Ca(OH)_{0.154}(CO_3)_{0.923} \bullet 0.997H_2O$ |
| d-A(B)CC (1h) | 15.70 & 0.36 | 49.53 | 15.70 | 1.48 | 82.82 | 47.52 | $Ca(OD)_{0.047}(CO_3)_{0.977} \bullet 1.028D_2O$ |

* Time for drying under rough vacuum is shown in parentheses. We assume a 100% H/D exchange in the d-A(B)CC sample at the time when TGA was performed (see sample descriptions below). However, the stoichiometry for d-A(B)CC is written as a deuterated expression.

† The residual weight for $CaO_{(s)}$ agrees with the calculated value within ± 2 wt.%.

## Supplementary Images:

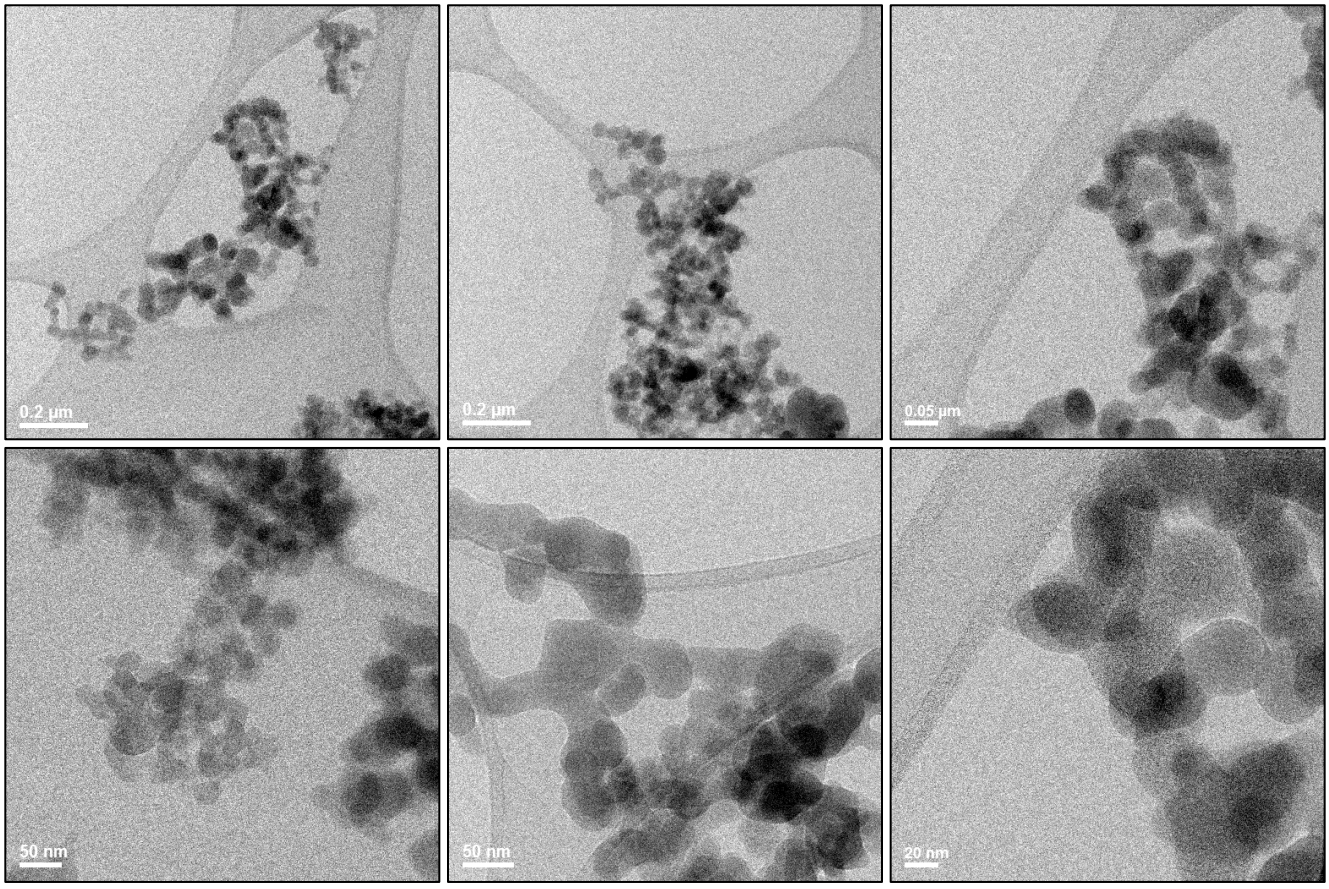


**Image S1.** Bright-field (S)TEM images of fresh protiated A(B)CC obtained by fast centrifugal mixing of cooled reactant materials, shown at various magnifications. A spherical morphology with a diameter of 30-60 nm is observed and agrees with other reported microscopy images.[10,12-13,15,20,22] **TEM:** (S)TEM images were acquired using a JEOL 2200FS aberration-corrected (S)TEM instrument, operated at 200 kV in STEM imaging mode with powder sample deposited directly onto a holey-carbon support film on a standard TEM grid.

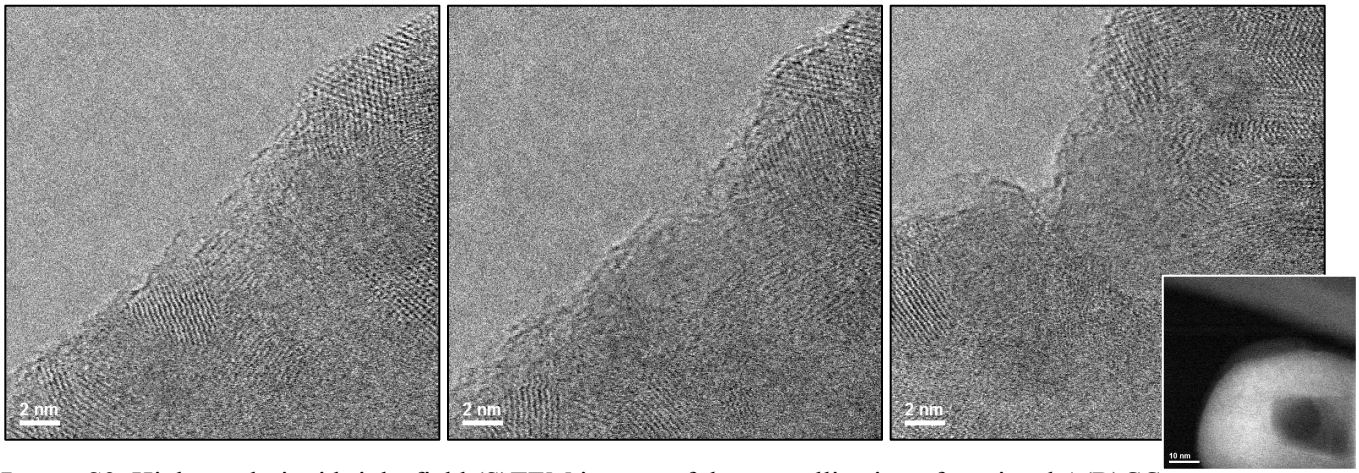


**Image S2.** High-resolutioni bright-field (S)TEM images of the crystallization of protiated A(B)CC as a consequence of electron beam effects and dehydration of originally hydrous material. From left to right, nearly sequential scanning images show the gradual changes in A(B)CC morphology and the appearance of crystalline ordered domains. Insert in lower right shows a low-magnification image of an A(B)CC particle with a hole created by the electron beam. A similar beam damage process has been described by Rodriguez-Blanco *et al.*[15]

**Supplementary Note:**

**Solution Preparation.** A fresh solution of 100 ml of a 50 mM $CaCl_2$ (pH = ~6.3 at ~24 °C) was prepared by dissolving 735 mg of $CaCl_2 \cdot 2H_2O$ (Sigma-Aldrich, ReagentPlus, ≥ 99%) in 100 mL MilliQ water, and was placed in a Teflon 500 mL centrifuge bottle. A second fresh solution of 50 mM $Na_2CO_3$ was prepared in an Erlenmeyer flask by dissolving 530 mg of $Na_2CO_3$ (Sigma-Aldrich, Anhydrous, 99.999%) in 100 mL of MilliQ water. To this solution 0.5 g NaOH was added (Sigma-Aldrich, ACS reagent, ≥ 97%, pellets), and the pH of the final $Na_2CO_3$-NaOH solution is ~12.9 at ~24 °C. To prepare deuterated products, $D_2O$ (Cambridge Iostope, 99.96% D), NaOD (ACROS Organics, 40wt.% in $D_2O$, 99+% D), and ethanol-D ($C_2H_5OD$, ACROS Organics, 99.5+% D) were used to replace chemicals containing H.

**Synthesis method: Rate of mixing is the key.** It is reasonable to expect that the solution conditions, practical levels of supersaturation, temperature, and pH, have a marked effect on the ion speciation and formation of pre-nucleation clusters (if present), and greatly influence the chemistry and formation kinetics of amorphous material obtained. Interaction with additives and reaction quenching/drying treatments might both stabilize certain prestructured forms and the corresponding variations in stability, crystallization kinetics, and other physical properties such as solubility. While attempting to reproduce previous work and upscale quantities synthesized, we noticed that the rate of mixing appeared to have a significant effect on the appearance of a crystalline fraction in the end product. Larger batches took longer to mix and the liquid remained more inhomogeneous for a longer time than when mixing smaller volumes. Building on insight from the titration method (Table S1) and the resulting $Ca^{2+}$ dosing curve presented,[19] the drop in free $Ca^{2+}$ concentration at the point of nucleation decreases with increasing pH of the carbonate solution. This suggests that the nucleation energy barrier gets smaller and nucleation events occur at faster rates as the system's pH increases. We hypothesized that if the formation of

A(B)CC is a process largely dominated by kinetics rather than thermodynamics, the rate of mixing might indeed have an effect on the material structure and on its stability. Consequently, at high pH conditions (necessary for gram quantities), a method providing an extremely rapid rate of mixing of reactant materials potentially could result in the formation of kinetically-trapped reactant products. This is not necessarily something easily achieved in a research chemistry laboratory where the rate of mixing of two solutions is essentially dictated by gravity, liquid viscosity, and operator skills - the latter being more difficult to control reproducibly.

In our fast centrifugal mixing method, the sudden rupture of the polyethylene film mixes the top solution into the bottom one at speeds of the order of tens of m/s, much faster than can be achieved by a human operator. A rough estimate of the speed of mixing can be given. If R is the radial position of the solution in the polyethylene sheet, d is the average separation of the two solutions, and Ω is the angular speed of the centrifuge, it will take a time $t = \arccos(R/(r+d))/\Omega$ for the polyethylene sheet solution to reach the solution at the bottom of the centrifuge bottle at a velocity $v = [(R+d)^2-R^2]^{1/2}/t$ (we neglect friction). If R= 10 cm, d= 5 cm, and Ω = 3500 rpm, then t = 2.3 ms and v = 49 m/s. Such rapid mixing cannot be achieved by a human operator mixing solutions in traditional laboratory glassware. The amount of time necessary for the steel ball to rupture the film can be altered by adjusting the film material and thickness and ball shape and mass to determine at which angular velocity of the centrifuge the film will rupture. A few tests with different films and steel balls of different sizes enabled a fast convergence on a protocol that worked well for our particular model of centrifuge and rotor. We noted here that this method for rapid mixing is quite general and could be applied to the preparation of other amorphous salts or kinetically trapped materials obtained by rapid reaction.

In the experimental setup, centrifugation was continued for 3-5 minutes, the supernatant liquid was poured out and the white-to-transparent material was rinsed with a few mL of ethanol (200 proof) at room temperature. The suspension in ethanol was filtered on a Buechner funnel (sealed-in fritted glass, 10-15 μm pore size) and then was dried at room temperature in a rough vacuum (~0.1 bar) for 1-2 h. The yield per batch was ~0.5 g. This method always resulted in an amorphous material, while conversion to calcite was reached within 3 days with samples simply stored at ambient conditions. Naturally, it is straightforward to vary a number of parameters such as temperature, pH, the starting concentration of the reacting solutions, and mixing rate. A deuterated product was prepared in the same manner with additional precautions, including: (i) a N2 filled glovebox was employed for solution preparation and sample handling; (ii) $CaCl_2$, $D_2O$, NaOD, and ethanol-D were used to replace chemicals containing H; (iii) centrifuge and filtration were completed outside of the glovebox (due to equipment size) but with effort to minimize time and exposure for isotopic exchange with atmospheric $H_2O$; and (iv) after filtration, sample was quickly transferred into the glovebox vacuum chamber for drying and storage.

**Synthetic A(B)CC Materials.** Three amorphous samples, two protiated (p-A(B)CC) and one deuterated (d-A(B)CC) materials, were independently synthesized using the method presented above. The two p-A(B)CC samples were dried for different time periods, 1 and 2 hours, respectively, and thus contain different amounts of $H_2O$ as confirmed later by thermogravimetric analysis (TGA). The d-A(B)CC sample was dried for 1 hour. In all cases purely amorphous structure was present 30 minutes after preparation as confirmed by laboratory powder X-ray diffraction (XRD). It is noted here that the H/D

isotopic exchange between $D_2O$ and atmospheric $H_2O$ in the deuterated sample is fairly rapid. Exchange is completed within 10 min (checked with infrared spectroscopy) after transferring a small amount of sample out of the glove box. Consequently, the ambient environment conditions for XRD and TGA mean that the deuterated sample as measured for these analysis techniques is chemically protiated.

**Powder X-ray diffraction and thermogravimetric analyses.** XRD patterns of fresh samples were measured within 30 min after drying. Sample powders were lightly pressed onto a zero-background quartz plate and were characterized using a PANalytical Empyrean X-ray diffractometer (Cu Kα radiation) with patterns recorded from 5º to 90º 2θ and counting for 0.185 sec at each 0.026º 2θ step, i.e., 10 min measurements. The d-A(B)CC sample (with H/D exchange) was rescanned after 24 and 48 hours and in all cases no crystalline peaks were observed. The composition of samples was determined by TGA using a TA5000IR instrument with a 10 °C/min heating rate to 800 °C (held isothermal for 2 min at the beginning), under a 25 mL/min argon gas flow.

**Synchrotron X-ray total scattering.** Data were collected utilizing a monochromatic high-energy beam (58.7 keV, 0.2114 Å) at the 11-ID-B beamline at the Advanced Photon Source, Argonne National Laboratory. The p-A(B)CC sample (prepared with 1 hour of drying) was loaded in 1 mm polyimide capillary, sealed with epoxy, and packed/shipped in an insulated cooler ~48 hours prior to measurement. Scattering data were measured in transmission mode at room temperature using a Perkin Elmer amorphous silicon image plate detector[23] for total of 30 min. Data for an empty polyimide container was also collected. The program Fit2D[24] was used to calibrate the sample to detector distance and detector alignment with data from a $CeO_2$ powder standard. Raw scattering data was integrated into Q-space spectra, applying a mask and polarization correction during integration. The total scattering structure factor S(Q) (Figure S1) were produced in PDFgetX2[25] by subtracting polyimide container scattering, utilizing the appropriate sample composition, and applying standard corrections for the area detector setup. Pair distribution function, PDF G(r), were calculated via Fourier transformation of the S(Q) data utilizing a $Q_{max}$ of 22.8 $Å^{-1}$. Reference data were also collected for water, monohydrocalcite (calcium carbonate monohydrate), aragonite and calcite.

**Neutron total scattering.** The d-A(B)CC sample was loaded/sealed in 5 mm quartz NMR tube inside the glove box and quickly transported to the beamline for neutron scattering measurements. The tube was loaded in the sample shifter carousel at the Nanoscale Ordered MAterials Diffractometer (NOMAD) instrument at the Spallation Neutron Source, Oak Ridge National Laboratory, as described by Neuefeind *et al.*[26] Scattering data were collected in 30 minute frames at room temperature in an Argon atmosphere for a total of 1.5 hours at 60 Hz setting. The beamline's autoreduction software[26] was used to normalize collected data, subtract background and container scattering signals, and produce histograms appropriate for PDF analysis. Inelastic-incoherent effects resulting from hydrogen contamination comprised a small portion of the sample-dependent background. This was corrected prior to Fourier transformation using the method of non-linear least-squares fitting to a pseudo-Voigt function. An absolute normalization was applied, i.e., the measured total scattering structure factor $S(Q)$ (Figure S1) was scaled to the corresponding sample compositions estimated based on TGA. Despite ~10% of H/D isotope exchange, the sample was found to remain deuterated, amorphous, and stable over the measurement period. Reference data were also collected for heavy water, monohydrocalcite (also

requiring hydrogen background correction), aragonite and calcite in quartz capillaries for one hour each. For H(D)-containing samples (p-A(B)CC, heavy water, and monohydrocalcite), a $Q_{max}$ of 25 Å$^{-1}$ was used, and for aragonite and calcite, a $Q_{max}$ of 36 Å$^{-1}$ was used.

In-situ thermal dehydration data were collected under continuous heating at a rate of 0.5 °C/min, and data were saved at 4 min increments, i.e., 2 °C temperature intervals. The total scattering data shown in a 2-D plot in Figure 2(a) (main text) are displayed with 2 °C temperature steps in each segment from ambient temperature to 450 °C. Figure S2 displays both 3-D and 2-D views of the same data set. During thermal dehydration, the sample can is not sealed and is exposed to a rough pumping/low vapor pressure condition.

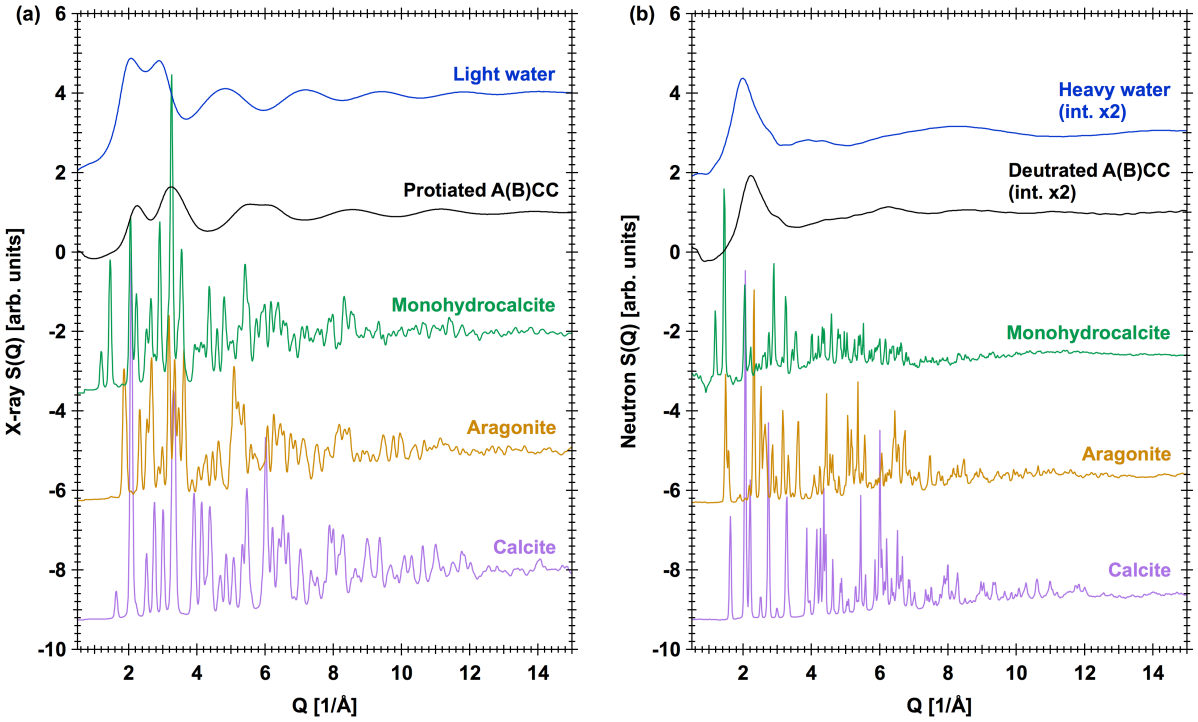


**Figure S1.** (a) X-ray and (b) neutron total scattering structure factor S(Q) of synthetically pure protiated and deuterated A(B)CC samples and three naturally occurring calcium carbonate minerals (monohydrocalcite, aragonite and calcite).

**Figure S2.** (a) 3-D and (b) 2-D plot of neutron total scattering structure factor S(Q) following the crystallization pathway of deuterated sample (d-A(B)CC).

**Comparison of local bonding characteristics of A(B)CC with reference materials**. By comparison with PDF of bulk water and calcium carbonate phases shown in Figure 3 (main text), peaks that can be readily interpreted are: (i) Peak 1: 0.97 Å H/D-$O_w$ bonds in $H_2O/D_2O$ molecules or $OH^-/OD^-$ species, (ii) Peak 2: 1.3 Å C-$O_c$ intramolecular bonds in $CO_3^{2-}$group, (iii) Peak 3: 1.58 Å H··H/D··D intramolecular distances in $H_2O/D_2O$ molecule, (iv) Peak 4: 2.2 Å $O_c$··$O_c$ intramolecular distances in $CO_3^{2-}$ group, and (v) Peak 5: 2.4 ± 0.2 Å Ca-$O_c$/$O_w$ bonds for the first coordination shell of $Ca^{2+}$. Peaks observed at distances > 3 Å reflect specific local structure arrangements. For instance, in light water, the ~2.8, 4.6, and 6.7 Å peaks are due mainly to intermolecular $O_w$··$O_w$ distances (H atoms do not contribute to significant degrees owing to their small scattering power for X-rays). In heavy water, the ~3.6 and 7.2 Å peaks are largely from intermolecular D··D and D··$O_w$ distances, according to Soper[27]. In crystalline phases of calcium

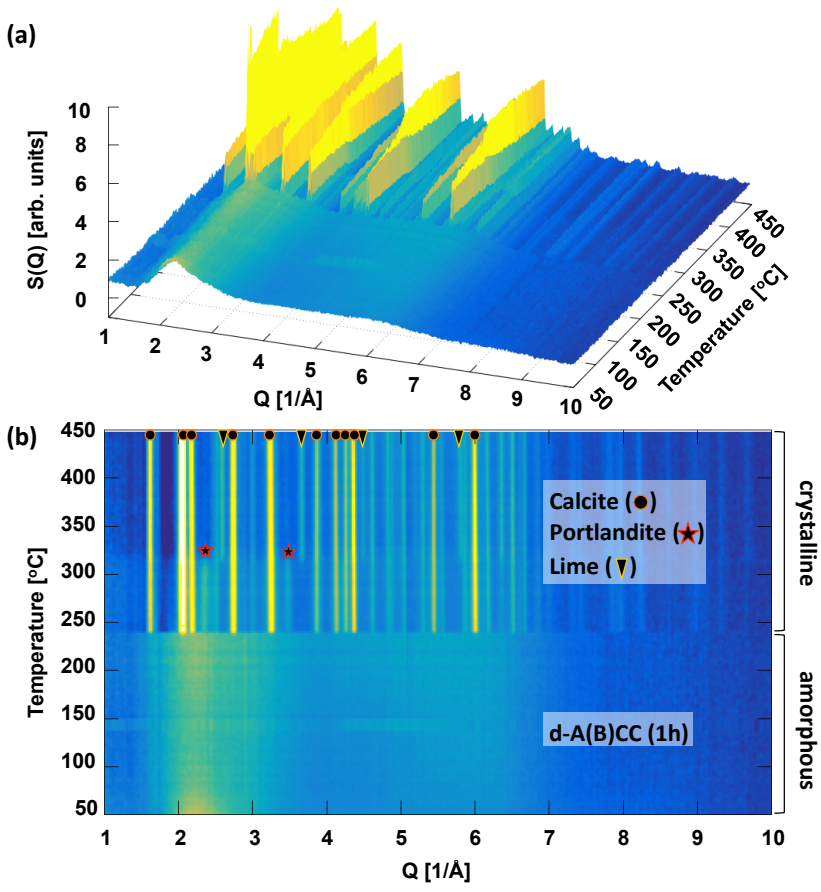

carbonate, higher length scale peaks can be assigned based on available structural models. To simplify the analysis, atomic structures of coordination spheres around $Ca^{2+}$ will be discussed below for each phase. In the calcite structure,[28] there are six $CO_3^{2-}$ groups bound to a $Ca^{2+}$ by each sharing one $O_c$ atom, i.e., all six $CO_3^{2-}$ are monodentate ligands. In such ordered $Ca^{2+}$ coordination spheres (coordination number of $Ca^{2+}$, $CN_{Ca}$, by $O_c$ is 6), the nearest-neighbor Ca··C and the second shell of Ca··$O_c$ and $O_c$··$O_c$ distances are all centered at ~3.2 Å (peaks 6 and 7). The nearest-neighbor Ca··Ca and the third shell of Ca··$O_c$ distances are located at ~4.2 Å (peak 8). The $Ca^{2+}$ in aragonite[29] is coordinated both monodentate (3) and bidentate (3) with a total of six $CO_3^{2-}$ groups around a $Ca^{2+}$, and thus the $CN_{Ca}$ by $O_c$ is 9 (note that aragonite is the densest, and highest pressure phase of calcium carbonate). Accordingly, the Ca-$O_c$ bonds of the first shell observed at ~ 2.5 Å (peak 5) are more spread out as compared to calcite. Furthermore, only the nearest-neighbor Ca··C and the second shell of $O_c$··$O_c$ distances are responsible for peaks 6 and 7. The second shell of Ca··$O_c$ and the nearest-neighbor Ca··Ca distances are located at ~4 Å (peak 8). A similar analysis can be applied to vaterite PDFs. Structures of vaterite reported have in general five to six $CO_3^{2-}$ groups bound to a $Ca^{2+}$, and depending on the orientational ordering of $CO_3^{2-}$, the $CN_{Ca}$ by $O_c$ in vaterite varies from 5 (ordered vaterite[30]: all 5 $CO_3^{2-}$ are monodentate) to 7 (disordered vaterite[31]: 5 monodentate and 1 bidentate). In the monohydrocalcite structure,[32] $Ca^{2+}$ are coordinated with four $CO_3^{2-}$ groups (2 monodentate and 2 bidentate) and two $H_2O$ molecules, yielding a $CN_{Ca}$ by $O_c$+$O_w$ of 8. The PDF peak at ~2.5 Å is thus due to Ca-$O_c$/$O_w$ bonds of the first shell (peak 5). Peaks 6 and 7 relate to the nearest-neighbor Ca··C and the second shell of $O_c$··$O_c$/$O_w$, distances. Note the formation of H-bonds, which are accepted by $O_c$, i.e., $O_c$··H-$O_w$. Peak 8 depicts the second shell of Ca··$O_c$/$O_w$ and nearest-neighbor Ca··Ca distances.

Since neutrons are sensitive to both light and heavy elements whereas in the studied system, X-rays are mainly sensitive to pairs containing Ca and O, the differences between the neutron and X-ray PDFs arise from C··O, C··C, and H/D··$x$ ($x$ = H/D, Ca, C, O) correlations in the neutron data. For instance, a negative scattering cross section of H (and pairs containing H) in protiated monohydrocalcite (p-MHC) has resulted in negative signals in the $r$-region of ~3-5 Å when comparing to deuterated monohydrocalcite (d-MCH) neutron PDF simulated using Swainson's structure[32] and simply switching D for H. For the direct comparison of A(B)CC to those of reference compounds, it is clear that neutron data provided more information than X-ray results. Further data analysis coupled with theoretical modeling and in situ thermal dehydration experiments utilizing the methods reported here is underway to provide a detailed picture of the amorphous structure, the role of hydrous components in the local structural ordering, and the interactions occurring during the amorphous-crystalline phase transitions of carbonate precipitates.

**Supplementary References**


1 Y. Kojima, A. Kawanobe, T. Yasue and Y. Arai, *J. Ceram. Soc. Jpn.*, 1993, **101**, 1145-1152.
2 N. Koga, Y. Nakagoe and H. Tanaka, *Thermochim. Acta*, 1998, **318**, 239-244.
3 J. Bolze, B. Peng, N. Dingenouts, P. Panine, T. Narayanan and M. Ballauff, *Langmuir*, 2002, **18**, 8364-8369.
4 A. L. Goodwin, F. M. Michel, B. L. Phillips, D. A. Keen, M. T. Dove and R. J. Reeder, *Chem. Mater.*, 2010, **22**, 3197-3205.
5 R. J. Reeder, Y. Tang, M. P. Schmidt, L. M. Kubista, D. F. Cowan and B. L. Phillips, *Cryst. Growth Des.*, 2013, **13**, 1905-1914.
6 F. M. Michel, J. MacDonald, J. Feng, B. L. Phillips, L. Ehm, C. Tarabrella, J. B. Parise and R. J. Reeder, *Chem. Mater.*, 2008, **20**, 4720-4728.
7 A. V. Radha, T. Z. Forbes, C. E. Killian, P. U. Gilbert and A. Navrotsky, *Proc. Natl. Acad. Sci. U.S.A.*, 2010, **107**, 16438-16443.
8 A. Fernandez-Martinez, B. Kalkan, S. M. Clark and G. A. Waychunas, *Angew. Chem. Int. Ed. Engl.*, 2013, **52**, 8354-8357.
9 A. V. Radha, A. Fernandez-Martinez, Y. Hu, Y.-S. Jun, G. A. Waychunas and A. Navrotsky, *Geochim. Cosmochim. Acta*, 2012, **90**, 83-95.
10 M. P. Schmidt, A. J. Ilott, B. L. Phillips and R. J. Reeder, *Cryst. Growth Des.*, 2014, **14**, 938-951.
11 D. J. Tobler, J. D. Rodriguez Blanco, H. O. Sørensen, S. L. S. Stipp and K. Dideriksen, *Cryst. Growth Des.*, 2016, DOI: 10.1021/acs.cgd.6b00630.
12 J. Ihli, A. N. Kulak and F. C. Meldrum, *Chem. Commun.*, 2013, **49**, 3134-3136.
13 J. D. Rodriguez-Blanco, S. Shaw, P. Bots, T. Roncal-Herrero and L. G. Benning, *J. Alloys Compd.*, 2012, **536**, S477-S479.
14 J. D. Rodriguez-Blanco, S. Shaw and L. G. Benning, *Nanoscale*, 2011, **3**, 265-271.
15 J. D. Rodriguez-Blanco, S. Shaw and L. G. Benning, *Mineral. Mag.*, 2008, **72**, 283-286.
16 J. Ihli, W. C. Wong, E. H. Noel, Y. Y. Kim, A. N. Kulak, H. K. Christenson, M. J. Duer and F. C. Meldrum, *Nat. Commun.*, 2014, **5**, 3169.
17 X.-R. Xu, A.-H. Cai, R. Liu, H.-H. Pan, R.-K. Tang and K. Cho, *J. Cryst. Growth*, 2008, **310**, 3779-3787.
18 M. Faatz, F. Gröhn and G. Wegner, *Adv. Mater.*, 2004, **16**, 996-1000.
19 D. Gebauer, A. Volkel and H. Colfen, *Science*, 2008, **322**, 1819-1822.
20 D. Gebauer, P. N. Gunawidjaja, J. Y. Ko, Z. Bacsik, B. Aziz, L. Liu, Y. Hu, L. Bergstrom, C. W. Tai, T. K. Sham, M. Eden and N. Hedin, *Angew. Chem. Int. Ed. Engl.*, 2010, **49**, 8889-8891.
21 D. L. Parkhurst, *User's quide to PHREEQE—a computer program for speciation, reaction-path, advective transport, and inverse geochemical calculations*, US Geological Survey Watere-Resources Investigations Report, 1995.
22 M. F. Khouzani, D. M. Chevrier, P. Güttlein, K. Hauser, P. Zhang, N. Hedin and D. Gebauer, *CrystEngComm*, 2015, **17**, 4842-4849.
23 P. J. Chupas, X. Qiu, J. C. Hanson, P. L. Lee, C. P. Grey and S. J. Billinge, *J. Appl. Crystallogr.*, 2003, **36**, 1342-1347.
24 A. P. Hammersley, S. O. Svensson, M. Hanfland, A. N. Fitch and D. Hausermann, *High Pressure Research*, 1996, **14**, 235-248.
25 X. Qiu, J. W. Thompson and S. J. L. Billinge, *J. Appl. Crystallogr.*, 2004, **37**, 678-678.
26 J. Neuefeind, M. Feygenson, J. Carruth, R. Hoffmann and K. K. Chipley, *Nuclear Instruments and Methods in Physics Research Section B: Beam Interactions with Materials and Atoms*, 2012, **287**, 68-75.

27 A. K. Soper, *ISRN Physical Chemistry*, 2013, **2013**, 1-67.
28 D. Graf, *Am. Mineral.*, 1961, **46**, 1283-1316.
29 S. M. Antao and I. Hassan, *Can. Mineral.*, 2009, **47**, 1245-1255.
30 A. Le Bail, S. Ouhenia and D. Chateigner, *Powder Diffr.*, 2011, **26**, 16-21.
31 R. Demichelis, P. Raiteri, J. D. Gale and R. Dovesi, *Cryst. Growth Des.*, 2013, **13**, 2247-2251.
32 I. P. Swainson, *Am. Mineral.*, 2008, **93**, 1014-1018.